Bioresource Technology 245 (2017) 1645–1654

Contents lists available at ScienceDirect

Bioresource Technology

journal homepage: www.elsevier.com/locate/biortech

Metabolic engineering of yeast for fermentative production of flavonoids

Angelica Rodriguez [a,1], Tomas Strucko [a,1], Steen Gustav Stahlhut [a], Mette Kristensen [a], Daniel Killerup Svenssen [a], Jochen Forster [a], Jens Nielsen [a,b], Irina Borodina [a,*]

[a] The Novo Nordisk Foundation Center for Biosustainability, Technical University of Denmark, Kemitorvet 220, 2800 Kgs Lyngby, Denmark
[b] Department of Biology and Biological Engineering, Chalmers University of Technology, Kemivägen 10, SE412 96 Gothenburg, Sweden

HIGHLIGHTS

- Flavonoids, natural secondary metabolites from plants, provide many health benefits.
- Six flavonoids were synthesized in yeast using glucose as sole carbon source.
- Resokaempferol and fisetin were synthesized in yeast for the first time.
- Flavonoids were synthesized via two precursor-supplying routes.
- Quercetin and kaempferol had the highest extracellular concentrations, up to 20–26 mg L^{-1}.

GRAPHICAL ABSTRACT

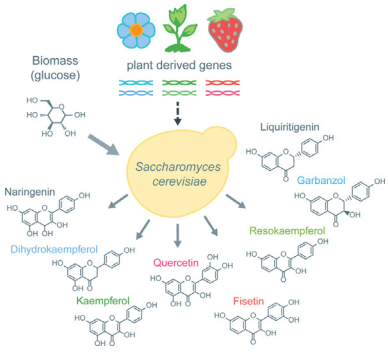

ARTICLE INFO

Article history:
Received 12 March 2017
Received in revised form 7 June 2017
Accepted 8 June 2017
Available online 12 June 2017

Keywords:
Flavonoids
Kaempferol
Resokaempferol
Fisetin
Saccharomyces cerevisiae

ABSTRACT

Yeast *Saccharomyces cerevisiae* was engineered for *de novo* production of six different flavonoids (naringenin, liquiritigenin, kaempferol, resokaempferol, quercetin, and fisetin) directly from glucose, without supplementation of expensive intermediates. This required reconstruction of long biosynthetic pathways, comprising up to eight heterologous genes from plants. The obtained titers of kaempferol 26.57 ± 2.66 mg L^{-1} and quercetin 20.38 ± 2.57 mg L^{-1} exceed the previously reported titers in yeast. This is also the first report of *de novo* biosynthesis of resokaempferol and fisetin in yeast.

The work demonstrates the potential of flavonoid-producing yeast cell factories.

1. Introduction

Flavonoids are aromatic secondary metabolites naturally synthesized by plants and fungi from aromatic amino acids L-phenylalanine and L-tyrosine. The structure of these phytochemicals is characterized by two phenolic rings and one heterocyclic ring. The main differences between flavonoids are related to the hydroxylation patterns, the position of the second aromatic ring and the saturation of the heterocyclic ring (Grotewold, 2006). Bioactive polyphenols such as flavonoids play a fundamental role in the physiology of plants; their natural functions include UV protection, reduction of oxidative damage in cells, and antibacterial effect (Cushnie and Lamb 2011).

Research on human cells showed positive properties of polyphenols in age-related diseases, cancer and cardiovascular diseases (Woelfle et al., 2010; Bulzomi et al., 2012). Moreover, some flavonoids, e.g., naringenin, have neuroprotective and antioxidant properties. Liquiritigenin has been reported as a protective agent

* Corresponding author.
E-mail address: irbo@biosustain.dtu.dk (I. Borodina).
[1] These authors contributed equally to this work.

http://dx.doi.org/10.1016/j.biortech.2017.06.043
0960-8524/

against oxidative stress in osteoblasts, and some liquiritigenin derivatives show antitumor and antidiabetic activity (Choi, 2012; Wedick et al., 2012; Liu et al., 2012; Raza et al., 2013; Hämäläinen et al., 2007). Kaempferol, quercetin and fisetin showed anti-cancer, cardio-protective and anti-inflammatory effects (Chou et al., 2013; Chen and Chen, 2013). Experiments with rats showed that doses of 50 mg kg^{-1} of quercetin inhibit the migration of melanoma cells. Other experiments with humans showed that doses of 150 mg day^{-1} of quercetin had positive effects on the health of people with high risk of cardiovascular disease (Caltagirone et al., 2000; Mukhtar et al., 2015). Fisetin has neuroprotective, neurotrophic and anti-amyloid properties, which makes it a promising therapeutic agent for neurodegenerative disorders such as Huntington and Alzheimer diseases (Maher et al., 2011; Currais et al., 2014).

The main obstacles for large-scale production of flavonoids from plant material are the long culture periods, requirements for specific cultivation conditions and low abundance. Additionally, extraction and purification processes add cost and result in product loss and degradation (Wang et al., 2011; Routray and Orsat, 2012). The concentration of flavonoids in different varieties and sources of fruits oscillate between 30 and 4000 mg kg^{-1} of dry weight (Hertog et al., 1992; Paganga et al., 1999; Miean and Mohamed, 2001; Crozier et al., 1997). This means that for the production of 1 kg of flavonoids, it is required to process 0.25–33 Tons of dry weight of fruits or vegetables.

Methods for phytochemicals extraction from agro-industrial waste have been developed in the recent years, and secondary metabolites such as carotenoids and flavonoids have been extracted from this feedstock (Matharu et al., 2016; Pfaltzgraff et al., 2013; Makris et al., 2007). Extraction of polyphenols such as flavonoids from waste is promising, however there are challenges that have to be overcome in terms of cost and optimization of extraction and purification methods (Mirabella et al., 2014; Luthria, 2012).

For a sustainable supply of phytochemicals, it can be an advantage to engage genetically engineered microbial cell factories, e.g., *E. coli* or *S. cerevisiae*. Koopman et al. (2012) reported production of 108.90 mg L^{-1} of naringenin from glucose using an engineered yeast strain. Furthermore, feeding naringenin to engineered cells allowed production of other flavonoids, such as genistein, kaempferol and quercetin (Trantas et al., 2009). Production of naringenin in *E. coli* reached 29 mg L^{-1} using glucose as carbon source, while kaempferol and quercetin have been produced using *p*-coumaric acid as precursor and fisetin using L-tyrosine as a precursor (Santos et al., 2011; Leonard et al., 2006; Stahlhut et al., 2015).

This study reports the development of a novel yeast cell factory for *de novo* production of flavonoids from glucose. The target flavonoids included: naringenin, liquiritigenin, kaempferol, resokaempferol, quercetin, and fisetin. Intermediate compounds and by-products were quantified to characterize regulated steps in the pathways and to identify targets for future improvements of the flavonoid-producing yeast cell factories.

2. Methods

2.1. Plasmid construction

The plasmids with biosynthetic pathways for flavonoids production were constructed using EasyClone 2.0 integrative plasmids with auxotrophic and dominant selection markers (Stovicek et al., 2015). The vectors integrate into well-defined integration sites previously described by (Mikkelsen et al. 2012).

The genes used for flavonoids production were: 4-coumaroyl-CoA ligase from *Petroselinum crispum* (*4CL*), chalcone synthase from *Petunia hybrida* (*CHS*), chalcone reductase from *Astragalus mongholicus* (*CHR*), chalcone isomerase from *Medicago sativa* (*CHI*), flavanone 3-hydroxylase from *Astragalus mongholicus* (*F3H*), flavonol synthase from *Arabidopsis thaliana* (*FLS*), cytochrome P450 reductase from *Catharanthus roseus* (*CPR*), a cytochrome P450 flavonoid monooxygenases from *Fragaria ananassa* and from *Petunia hybrida* (*FMO*) (Fig. 1). All the genes were synthesized by GeneArt (LifeTechnologies) in codon-optimized versions for *E. coli* as stated in Stahlhut et al. (2015).

DNA fragments (BioBricks), encoding genes or promoters, were amplified by PCR using primers and templates as described in Table 1. Individual BioBricks were assembled into the integrative plasmids by USER cloning as described previously (Stovicek et al., 2015). Finally, the resulting vectors (Table 2) were verified by sequencing.

2.2. Strain construction

For expression of flavonoid biosynthetic pathways, in this research were employed three *S. cerevisiae* strains, engineered to produce *p*-coumaric acid (Table 3). The ST4757 strain was engineered to produce *p*-coumaric acid using the phenylalanine ammonia-lyase (PAL) pathway and the strains ST4069 and ST2645 produced *p*-coumaric acid via the tyrosine ammonia-lyase (TAL) pathway. To obtain flavonoid production, the strains were transformed with *Not*I-linearized integrative vectors carrying pathway genes via lithium acetate protocol (Gietz and Woods, 2002). The transformants were selected on synthetic drop-out medium (Sigma-Aldrich), selecting for *URA3*, *HIS5* and *LEU2* markers. For selection on acetamide, the media contained 0.17 % yeast nitrogen base without amino acids and ammonium sulfate and 6.6 g L^{-1} of potassium sulfate and 0.6 g L^{-1} acetamide. For selection of dominant markers *NatMX*, *KanMX*, *BleMX* or *HphMX*, the medium was supplemented with 100 mg L^{-1} nourseothricin, 200 mg L^{-1} G418 disulfate salt, 10 mg L^{-1} phleomycin or 200 mg L^{-1} hygromycin B respectively. Correct integration of the vectors was verified by yeast colony PCR. The yeast strains constructed in this study are listed in Table 3.

2.3. Media and cultivations

For selection of yeast transformants and for routine cultivations, synthetic complete (SC) medium as well as drop-out media (SC-Ura, SC-Leu, SC-His) and agar plates were prepared using premixed drop-out powders from Sigma-Aldrich. Synthetic fed-batch medium for *S. cerevisiae* M-Sc.syn-1000 (FIT) was purchased from M2P Labs GmbH (Germany). The medium was supplemented with vitamins solution (final 1% v/v) and the enzyme mix (final concentration 0.5% v/v) immediately before use.

For the quantification of production of flavonoids for each strain, five single colonies originating from independent transformants were tested. The colonies were inoculated in 0.5 ml drop-out SC liquid medium without uracil, histidine, and/or leucine in 96-deep well microtiter plates with air-penetrable lid (EnzyScreen, The Netherlands). The plates were incubated at 30 °C with 250 rpm agitation at 5 cm orbit cast overnight. 50 μl of the overnight cultures were used to inoculate 0.5 ml synthetic fed-batch medium in a 96-deep well plate. Fermentation was carried out for 72 h at the same conditions as before. At the end of cultivation, samples for metabolite analysis and optical density (OD) were taken. OD_{600} was estimated as follows: 10 μl of fermentation broth was mixed with 190 μl water in a 96 well microtiter plate and absorbance was measured at 600 nm wavelength in microplate reader BioTek Synergy MX (BioTek). 200 μl of the culture were mixed with 200 μl of absolute ethanol, the mixture was centrifuged at 2272*g*

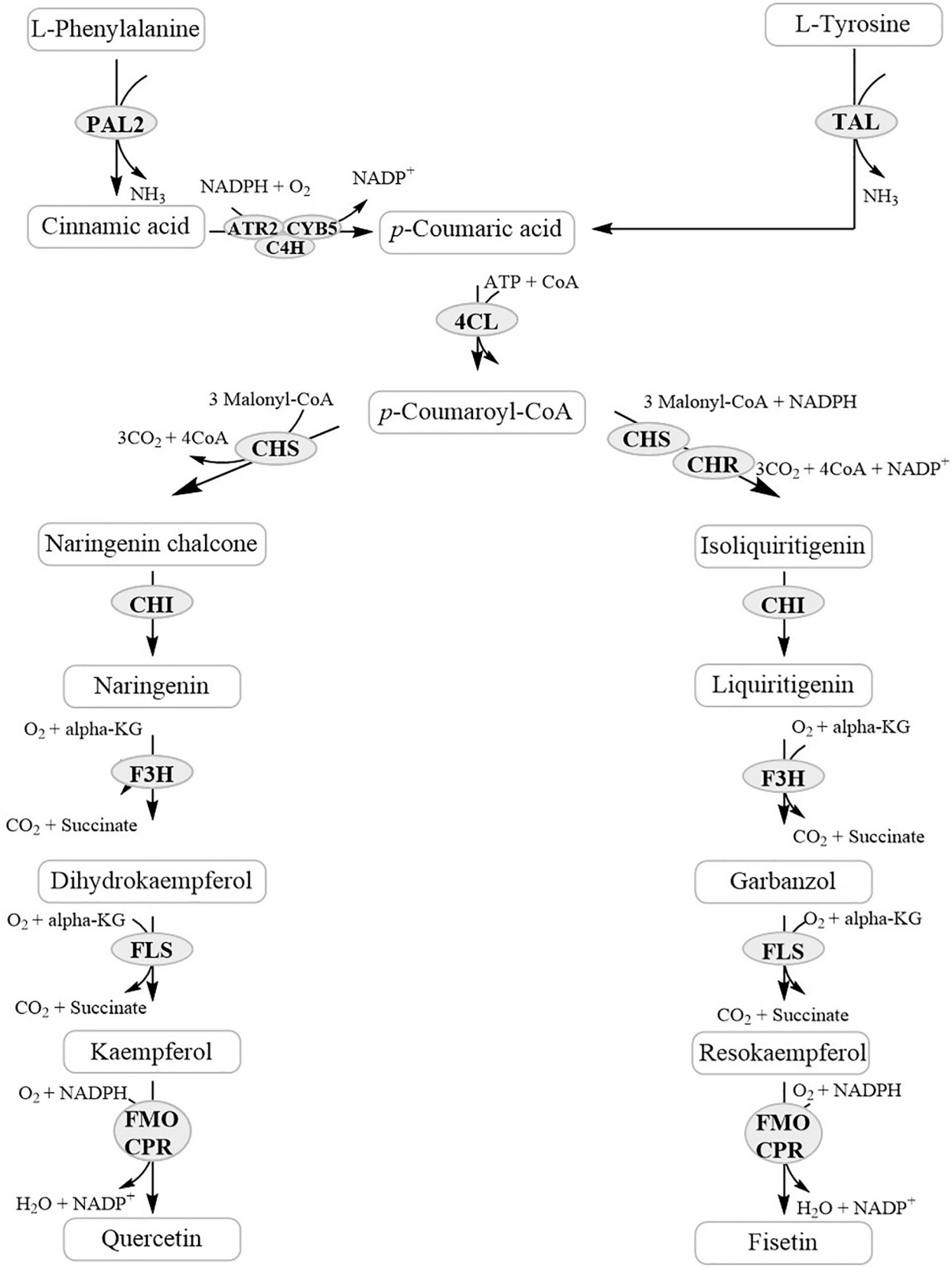

Fig. 1. Flavonoid biosynthetic pathways engineered into yeast *S. cerevisiae*. *PAL2*: phenylalanine ammonia-lyase; *C4H*: cinnamate 4-hydroxylyase; *ATR2* cytochrome p450 reductase; *CYB5*: cytochrome b5 electron carrier; *TAL*: tyrosine ammonia-lyase; *4CL*: 4-coumaroyl-CoA ligase; *CHS*: chalcone synthase; *CHR:* chalcone reductase; *CHI*: chalcone isomerase; *F3C*: flavanone 3-hydroxylase; *FLS*: flavonol synthase; *FMO*: flavonoid 3′-monooxygenase; *CPR*: cytochrome P450 reductase; alpha-KG: alpha-ketoglutarate.

Table 1
Primers used in this study and list of Biobricks generated by PCR amplification, description of the templates can be found in Stahlhut et al. (2015).

PRIMERS		
USER cloning		
ID	Name	Sequence (5′-3′)
7628	Pc_4Cl_U2_fw	ATCTGTCAUAAAACAATGGGAGACTGTGTAGCAC
7629	Pc_4Cl_U2_rv	CACGCGAUTCATTATTTGGGAAGATCACCGGATG
7632	Ph_CHS_U1_fw	AGTGCAGGUAAAACAATGACCATGGTTACCGTTGAAG
7633	Ph_CHS_U1_rv	CGTGCGAUTCATTAGGTTGCAACGCTATGCAG
7636	Ms_CHI_U1_fw	AGTGCAGGUAAAACAATGACCATGGCAGCAAGC
7637	Ms_CHI_U1_rv	CGTGCGAUTCATTAGTTGCCGATTTTAAAGGCACC
7640	Ms_CHR_U2_fw	ATCTGTCAUAAAACAATGACCATGGGTAGCGTTG
7641	Ms_CHR_U2_rv	CACGCGAUTCATTAGTCATCATACAGATCATTCAGACC
7644	At_F3H_U2_fw	ATCTGTCAUAAAACAATGGCTCCAGGAACTTTGAC
7645	At_F3H_U2_rv	CACGCGAUTCACTAAGCGAAGATTTGGTCGACAG
7648	At_FLS_U1_fw	AGTGCAGGUAAAACAATGGAGGTCGAAAGAGTCC
7649	At_FLS_U1_rv	CGTGCGAUTCATCAATCCAGAGGAAGTTTATTGAGC
7654	Fa_FMO-Cr_CPR_U1_fw	AGTGCAGGUAAAACAATGGCGATTACCCTGCTG
7655	Fa_FMO-Cr_CPR_U1_rv	CGTGCGAUTCATTACCAAACGTCACGCAGATAAC
7658	Ph_FMO-Cr_CPR_U1_fw	AGTGCAGGUAAAACAATGGCGATTCTGTATACCGTG
7659	Ph_FMO-Cr_CPR_U1_rv	CGTGCGAUTCATTACCAAACGTCACGCAGATAAC
Verification		
ID	*Name*	*Sequence (5′-3′)*
892	Sc_XII-1-down-out-sq	GGACGACAACTACGGAGGAT
894	Sc_XII-2-down-out-sq	GGCCCTGATAAGGTTGTTG
900	Sc_XII-5-down-out-sq	GTGGGAGTAAGGGATCCTGT
2220	Sc_Colo_pcr_fw	CCTGCAGGACTAGTGCTGAG
8419	Sc_XI-5_down-out-sq	GCATGGTCACCGCTATCAGC

BIOBRICKS			
Name	*Template for PCR*	*Fw primer for PCR*	*Rv primer for PCR*
BB0653 (Pc_4Cl→)	pCDF-4cl-2Pc	ID7628 (Pc_4Cl_U2_fw)	ID7629 (Pc_4Cl_U2_rv),
BB0655(Ph_CHS←)	pET-chsPh-chiMs	ID7632 (Ph_CHS_U1_fw)	ID7633 (Ph_CHS_U1_rv)
BB0656 (Ms_CHI←)	pET-chsPh-chiMs	ID7636 (Ms_CHI_U1_fw)	ID7637 (Ms_CHI_U1_rv)
BB0658 (Am_CHR→)	pRSF-chrAm	ID7642 (Am_CHR_U2_fw)	ID7643 (Am_CHR_U2_rv)
BB0659 (At_F3H→)	pCDFf3hAt-fls-1At	ID7644 (At_F3H_U2_fw)	ID7645 (At_F3H_U2_rv)
BB0660 (At_FLS←)	pCDFf3hAt-fls-1At	ID7648 (At_FLS_U1_fw)	ID7649 (At_FLS_U1_rv)
BB0661 (Fa_FMO-Cr_CPR←)	pACYCf30hFxa2-cprCr	ID7654 (Fa_F3H-Cr_CPR_U1_fw)	ID7655 (Fa_F3H-Cr_CPR_U1_rv)
BB0680 (Ph_FMO-Cr_CPR←)	pACYCf30hPh-cprCr	ID7658 (Ph_F3H-Cr_CPR_U1_fw)	ID7659 (Ph_F3H-Cr_CPR_U1_rv)

Table 2
Plasmids used in this study.

Plasmid ID	Genotype	Source
Parental integrative plasmids		
pCfB2399	pXI-5-lox P-amdSYMsyn, P_{TEF1}-T_{ADH1}, P_{PGK1}-T_{CYC1}	Stovicek et al. (2015)
pCfB2197	pXII-1-lox P-NatMXsyn3, P_{TEF1}-T_{ADH1}, P_{PGK1}-T_{CYC1}	Stovicek et al. (2015)
pCfB2225	pXII-2-lox P-KanMXsyn, P_{TEF1}-T_{ADH1}, P_{PGK1}-T_{CYC1}	Stovicek et al. (2015)
pCfB2337	pXII-5-lox P-HPHMXsyn, P_{TEF1}-T_{ADH1}, P_{PGK1}-T_{CYC1}	Stovicek et al. (2015)
pCfB2224	pXI-2-lox P-KanMXsyn, P_{TEF1}-T_{ADH1}, P_{PGK1}-T_{CYC1}	Stovicek et al. (2015)
pCfB2855	pXII-2-lox P-amdSYM, P_{TEF1}-T_{ADH1}, P_{PGK1}-T_{CYC1}	Stovicek et al. (2015)
Integrative plasmids for pathway expression		
pCfB0848	pXI-2-loxP-URA3, P_{TEF1}-*CYB5* T_{ADH1}, P_{PGK1}-*ATR2*-T_{CYC1}	Li et al. (2016)
pCfB1018	pXI-5-loxP-HIS5, P_{TEF1}-*PAL2*-T_{ADH1}, P_{PGK1}-*C4H* T_{CYC1}	Li et al. (2016)
pCfB3437	pXI-5-lox P-amdSYMsyn, P_{TEF1}-Ph_*CHS*-T_{ADH1}, P_{PGK1}-Pc_*4CL*-T_{CYC1}	This study
pCfB2879	pXII-1-lox P-NatMXsyn3, P_{TEF1}-Ms_*CHI*-T_{ADH1}, P_{PGK1}-Am_*CHR*-T_{CYC1}	This study
pCfB2893	pXII-1-lox P-NatMXsyn3, P_{TEF1}-Ms_*CHI*-T_{ADH1}	This study
pCfB3643	pXII-2-lox P-KanMXsyn, P_{TEF1}-At_*FLS*-T_{ADH1}, P_{PGK1}-At_*F3H*-T_{CYC1}	This study
pCfB3654	pXII-5-lox P-HPHMXsyn, P_{TEF1}-Ph_*FMO*-Cr_*CPR*-T_{ADH1}	This study
pCfB3655	pXII-5-lox P-HPHMXsyn, P_{TEF1}-Fa_*FMO*-Cr_*CPR*-T_{ADH1}	This study
pCfB4753	pXII-2-lox P-amdSYM, P_{TEF1}-Ph_*CHS*-T_{ADH1}, P_{PGK1}-Pc_*4CL*-T_{CYC1}	This study
pCfB4754	pXI-2-lox P-KanMXsyn, P_{TEF1}-At_*FLS*-T_{ADH1}, P_{PGK1}-At_*F3H*-T_{CYC1}	This study
pCfB4856	pXII-4-lox P-BleSyn, P_{TEF1}-Ph_*CHS*-Am_*CHR*-T_{ADH1}	This study
pCfB4857	pXII-4-lox P-BleSyn, P_{TEF1}-Ph_*CHS*-T_{ADH1}, P_{PGK1}-Am_*CHR*-T_{CYC1}	This study

for 15 min and 250 μl of supernatant were analyzed for flavonoids concentration by HPLC.

2.4. Quantification and identification of flavonoids

Quantification of flavonoids was performed on a Dionex Ultimate 3000 HPLC equipped with a Discovery HS F5 150 mm × 4.6 mm column (particle size 5 μm) connected to a UV detector (277, 290, 333 and 370 nm). Samples were analyzed using a gradient method with two solvents: 10 mM ammonium formate pH 3.0 (A) and acetonitrile (B). For *p*-coumaric acid, naringenin and liquiritigenin detection, a flow rate of 1.5 ml min^{-1} was used. The program started with 5% of solvent B (0–0.5 min), after which its fraction was increased linearly from 5% to 60% (0.5–7 min), then the fraction was maintained at 60% (7–9.5 min), after that the fraction was decreased from 60% to 5% (9.5–9.6 min), finally, the fraction was maintained at 5% (9.6–12 min). *p*-Coumaric acid was detected at 5.6 min (333), liquiritigenin at 6.8 (277) and naringenin at 7.5 min (290 nm). For kaempferol, resokaempferol, quercetin and fisetin detection, a flow rate of 1.5 ml min^{-1} was used. The program started with 20% of solvent B (0–2 min), after which its fraction was increased linearly from 20% to 45% (2–20 min), then the fraction was decreased from 45% to 20% (20–22 min) and maintained at 20% for 2 min (22–24 min). Fisetin was detected at 10.3 min (333 nm), liquiritigenin at 12.8 min (277 nm), resokaempferol at 13.3 min (370 nm) and quercetin at 13.9 min (370 nm).

The pure compounds *p*-coumaric acid (≥98.0%), naringenin (98%), kaempferol (≥97.0%), quercetin (≥97.0%) and fisetin (≥98.0%) were purchased from Sigma Aldrich Co. (Denmark); liquiritigenin (≥98.0%) was purchased from Tocris Bioscience (United Kingdom) and resokaempferol (≥95.0%) was purchased from Extrasynthese (France). The compounds were used to generate calibration curves; the areas were integrated with Chromeleon 7 and used for quantification. The flavonoids were identified by comparing the retention times and UV absorbance spectra of the samples with authentic compounds. For all the strains five biological replicates were analyzed.

2.5. Identification of fisetin

For fisetin identification, the samples were dried at room temperature under reduced pressure using a Centrifugal Vacuum Concentrator (Savant Speed Vacs Concentrator, Thermofisher Scientific, Waltham Ma), followed by reconstitution using a 0.1% solution of formic acid in LC-MS grade acetonitrile. 20 μl of each sample were then injected and analyzed on a Dionex UltiMate 3000 UHPLC (Thermo Fisher Scientific, San Jose, CA) connected to an Orbitrap Fusion Mass Spectrometer (Thermo Fisher Scientific, San Jose, CA). The UHPLC used a Supelco Discovery HS F5-3, 15 cm × 2.1 mm, 3 μm column. Temperature was 30 °C and flow rate was 0.6 mL/min with a mobile phase of 95% 0.1 % formic acid (mobile phase A) and 5% acetonitrile with 0.1% formic acid (mobile phase B) for 2 min followed by a linear gradient to 95% mobile phase B over 12 min. This gradient was held for 2 min after which it was changed immediately to 95% mobile phase A and 5% mobile phase B and held for 6 min. The sample was passed on to the MS equipped with a heated electrospray ionization source (HESI) in a positive-ion mode with nitrogen as nebulizer gas (52 a.u.). The cone and probe temperatures were 356 °C and 420 °C, respectively. Probe gas flow was 16 a.u. and spray voltage was 3500 V. Scan range was 150–1000 Da and time between scans was 100 ms.

3. Results and discussion

3.1. Flavonoids pathway design

Previously, Stahlhut et al. reported reconstruction of a biosynthetic pathway for the production of fisetin from L-tyrosine in *E. coli* (Fig. 1) (Stahlhut et al., 2015). This study aimed to develop a fermentation process for *de novo* production of a portfolio of related flavonoids from a cheap carbon source and using yeast *S. cerevisiae* as the host. The biosynthetic pathway towards flavonoids is depicted in Fig. 1. The precursor, *p*-coumaric acid, was synthesized either from L-tyrosine via tyrosine ammonia-lyase (TAL) or from L-phenylalanine by the use of phenylalanine ammonia-lyase (PAL). First, *p*-coumaric acid must be activated by a 4-coumaroyl-CoA ligase *4CL*, and for this a variant from *P. crispum* was used. Next, chalcone synthase *CHS* from *P. hybrida* and chalcone isomerase *CHI* from *M. sativa* were used to convert the resulting *p*-coumaroyl-CoA and three molecules of malonyl-CoA into naringenin. To obtain isoliquiritigenin, chalcone reductase *CHR* from *A. mongholicus* was additionally overexpressed. The resulting naringenin and isoliquiritigenin producing strains were further engineered towards production of respectively kaempferol and resokaempferol by overexpression of flavanone 3-hydroxylase

Table 3
Strains used in this study.

Platform strains producing *p*-coumaric acid				
Strain ID	Genotype			Source
ST4069	*Mata* P_{TEF1} → Fj_*TAL*			Rodriguez et al. (2015)
ST2645	*Mata* P_{TEF1} → Fj_*TAL*, P_{TEF1} → Sc_*ARO7*^{G141S}, P_{PGK1} → Sc_*ARO4*^{K229L}, *Δaro10 Δpdc5*			Rodriguez et al. (2015)
ST4757	*Matα* P_{TEF1} → *PAL2*, P_{PGK1} → *C4H*, P_{PGK1} → *CYB5*, P_{TEF1} → *ATR2*			This study
Strains transformed with integrative plasmids				
Strain ID	Parent strain	Integrated plasmids	Integrated flavonoid pathway genes	Source
ST5066	ST4069	pCfB3437, pCfB2893	P_{PGK1} → *4CL*, P_{TEF1} → *CHS*, P_{TEF1} → *CHI*	This study
ST5067	ST4069	PCFB343, pCfB2879	P_{PGK1} → *4CL*, P_{TEF1} → *CHS*, P_{TEF1} → *CHI*, P_{PGK1} → *CHR*	This study
ST5068	ST2645	PCfB3437, pCfB2893	P_{PGK1} → *4CL*, P_{TEF1} → *CHS*, P_{TEF1} → *CHI*	This study
ST5069	ST2645	PCfB3437, pCfB2879	P_{PGK1} → *4CL*, P_{TEF1} → *CHS*, P_{TEF1} → *CHI*, P_{PGK1} → *CHR*	This study
ST5070	ST5068	pCfB3643	P_{PGK1} → *4CL*, P_{PGK1} → *CHS*, P_{TEF1} → *CHI*, P_{PGK1} → *F3H*, P_{TEF1} → *FLS*	This study
ST5071	ST5069	pCfB3643	P_{PGK1} → *4CL*, P_{TEF1} → *CHS*, P_{TEF1} → *CHI*, P_{PGK1} → *F3H*, P_{TEF1} → *FLS*	This study
ST5072	ST5070	pCfB3654	P_{PGK1} → *4CL*, P_{TEF1} → *CHS*, P_{TEF1} → *CHI*, P_{PGK1} → *F3H*, P_{TEF1} → *FLS*, P_{TEF1} → *Fa_FMO CPR*	This study
ST5073	ST5070	pCfB3655	P_{TEF1} → *4CL*, P_{TEF1} → *CHS*, P_{TEF1} → *CHI*, P_{PGK1} → *F3H*, P_{TEF1} → *FLS*, P_{TEF1} → *Ph_FMO-CPR*	This study
ST5074	ST5071	pCfB3654	P_{PGK1} → *4CL*, P_{TEF1} → *CHS*, P_{TEF1} → *CHI*, P_{PGK1} → *CHR*, P_{PGK1} → *F3H*, P_{TEF1} → *FLS*, P_{TEF1} → *Fa_FMO-CPR*	This study
ST5075	ST5071	pCfB3655	P_{PGK1} → *4CL*, P_{TEF1} → *CHS*, P_{TEF1} → *CHI*, P_{PGK1} → *CHR*, P_{PGK1} → *F3H*, P_{TEF1} → *FLS*, P_{TEF1} → *Ph_FMO-CPR*	This study
ST4972	ST4757	PCfB4753, PCfB4754, PCfB2879, PCfB3654	P_{PGK1} → *4CL*, P_{TEF1} → *CHS*, P_{TEF1} → *CHI*, P_{PGK1} → *CHR*, P_{PGK1} → *F3H*, P_{TEF1} → *FLS*, P_{TEF1} → *Ph_FMO-CPR*	This study
ST5401	ST5074	pCfB4856	P_{TEF1} → *CHS-CHR (fusion)*	This study
ST5402	ST5074	pCfB4587	P_{TEF1} → *CHS*, P_{PGK1} → *CHR*	This study

F3H from *A. mongholicus* and flavonol synthase *FLS* from *A. thaliana*. Lastly, two different cytochrome P450 flavonoid monooxygenases *FMOs*, one from *F. ananassa* and another from *P. hybrida*, were overexpressed in the kaempferol-producing strain to obtain quercetin and in the resokaempferol-producing strain to obtain fisetin. Each of the tested *FMOs* was fused in-frame with cytochrome P450 reductase *CPR* from *C. roseus*.

3.2. Biosynthesis of naringenin and liquiritigenin

To begin with, two platform strains, producing low or high amounts of *p*-coumaric acid, were explored for their capacity to make naringenin and liquiritigenin. Strain ST4069, which produced 0.24 ± 0.03 g L^{-1} of *p*-coumaric acid in the previous study, was employed as the low-producer, while strain ST2645, which reached a titer of 1.93 ± 0.26 g L^{-1}, was used as the high-producer (Rodriguez et al., 2015). Strain ST4069 has overexpression of a *TAL* gene, while strain ST2645 has additional modifications increasing the flux towards aromatic amino acids: knock-outs of *ARO10* and *PDC5* genes and over-expressions of *ARO4*^{fbr} and *ARO7*^{fbr}. To obtain naringenin production, 4-coumaroyl-CoA ligase *4CL*, chalcone synthase *CHS* and chalcone isomerase *CHI* were overexpressed. For liquiritigenin production, chalcone reductase *CHR* was additionally overexpressed. The titers of naringenin and liquiritigenin were ca. 3-fold higher in the strain background with optimized *p*-coumaric acid production, reaching 1.55 ± 0.13 mg L^{-1} of naringenin and 5.31 ± 0.48 mg L^{-1} of liquiritigenin. *p*-Coumaric acid accumulated in the medium, particularly in the optimized strains, where up to 8 mg L^{-1} of *p*-coumaric acid were measured. Naringenin (~1 mg L^{-1}) also accumulated alongside liquiritigenin, indicating incomplete reduction by CHR (Fig. 2A–D).

3.3. Biosynthesis of kaempferol and resokaempferol

The naringenin- (strain ST5068) and liquiritigenin- (strain ST5069) producing strains were further engineered for production of respectively kaempferol and resokaempferol by overexpressing the genes encoding flavanone 3-hydroxylase *F3H* and flavonol synthase *FLS*. As a result, two new strains were obtained, strain ST5070 for the production of kaempferol and strain ST5071 for the production of resokaempferol. Strain ST5070 produced 26.57 ± 2.66 mg L^{-1} of kaempferol as well as two pathway intermediates: 10.75 ± 0.87 mg L^{-1} of *p*-coumaric acid and 0.83 ± 0.05 of naringenin (Fig. 2E). The high titer of kaempferol was surprising, considering that the parent strain produced less than 2 mg L^{-1} of kaempferol precursor, naringenin. The depletion of naringenin and higher capacity to produce kaempferol imply that the conversion steps of naringenin into kaempferol are very efficient. The resokaempferol producing strain (ST5071) accumulated 0.51 ± 0.03 mg L^{-1} of resokaempferol, 14.54 ± 1.96 mg L^{-1} of *p*-coumaric acid, 11.39 ± 0.33 mg L^{-1} of kaempferol, and less than 1 mg L^{-1} of naringenin and liquiritigenin (Fig. 2F). In the resokaempferol strain, by-product kaempferol was produced, which results from incomplete reduction of *p*-coumaroyl-CoA by CHR.

3.4. Biosynthesis of fisetin and quercetin

For the production of quercetin and fisetin, it is necessary to overexpress cytochrome P450 flavonoid monooxygenase (*FMO*) and cytochrome P450 reductase (*CPR*). In this study, two *FMO* variants were evaluated, one from *F. ananassa* and another from *P. hybrida*. Each FMO was fused in-frame to the *CPR* from *C. roseus* by a flexible glycine-serine linker (5′-GGGTCGAC-3′).

The genes were overexpressed in the kaempferol producing strain (ST5068) to obtain 16.04 ± 0.37 mg L^{-1} and 20.38 ± 2.57 mg L^{-1} of quercetin in the strains with *FMO* from *F. ananassa and P. hybrida* respectively (Fig. 2G and I). For fisetin biosynthesis, the host strain was the strain engineered for resokaempferol production (ST5069). Upon overexpression of *FMO-CPR* fusions, 1.20 ± 0.19 mg L^{-1} and 1.65 ± 0.10 mg L^{-1} of fisetin was obtained respectively (Fig. 2H and J). The strains overexpressing the *FMO* of *F. ananassa* additionally accumulated kaempferol and naringenin, while the strains with *FMO* from *P. hybrida* did not secrete these intermediates, hence the latter strain (ST5074) was chosen for further work. Fisetin was detected when expressing both the *FMO* from *F. ananassa* and *P. hybrida*. The observed ion 287 in positive mode is congruent with the ions recognized in the fisetin standard. The spectra for the infusion of the fisetin standard gave an ion with *m*/*z* 287.0549, which corresponds to 0.35 ppm of ion with the ionic formula of C15H11O6 in positive ion mode;

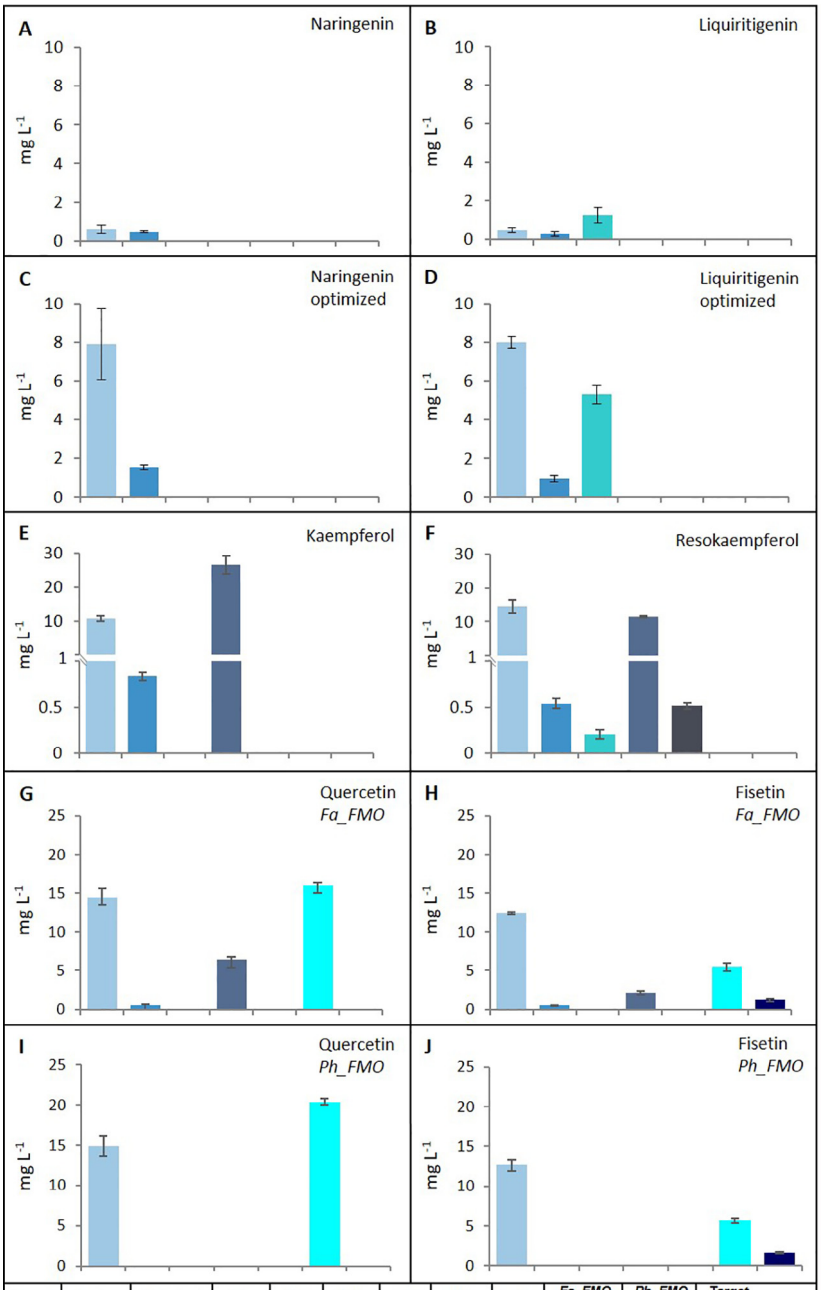

Panel	Strain	Optimized	4CL	CHS	CHI	CHR	F3H	FLS	Fa_FMO CPR	Ph_FMO CPR	Target compound
A	ST5066	-	+	+	+	-	-	-	-	-	Naringenin
B	ST5067	-	+	+	+	+	-	-	-	-	Liquiritigenin
C	ST5068	+	+	+	+	-	-	-	-	-	Naringenin
D	ST5069	+	+	+	+	+	-	-	-	-	Liquiritigenin
E	ST5070	+	+	+	+	-	+	+	-	-	Kaempferol
F	ST5071	+	+	+	+	+	+	+	-	-	Resokaempferol
G	ST5072	+	+	+	+	-	+	+	+	-	Quercetin
H	ST5073	+	+	+	+	+	+	+	+	-	Fisetin
I	ST5074	+	+	+	+	-	+	+	-	+	Quercetin
J	ST5075	+	+	+	+	+	+	+	-	+	Fisetin

Fig. 2. Strains engineered for biosynthesis of flavonoids via TAL pathway. A. Naringenin pathway expressed in low-level *p*-CA strain ST4069. B. Liquiritigenin pathway expressed in low-level *p*-CA strain ST4069. C. Naringenin pathway expressed in high-level *p*-CA strain ST2645. D. Liquiritigenin pathway expressed in high-level *p*-CA strain ST2645. E. Kaempferol pathway expressed in high-level *p*-CA strain ST2645. F. Resokaempferol pathway expressed in high-level *p*-CA strain ST2645. G. Quercetin pathway expressed in high-level *p*-CA strain ST2645; flavonoid 3′-monooxygenase (*FMO*) from *F. ananassa*. H. Fisetin pathway expressed in high-level *p*-CA strain ST2645; flavonoid 3′-monooxygenase (*FMO*) from *F. ananassa*. I. Quercetin pathway expressed in high-level *p*-CA strain ST2645; flavonoid 3′-monooxygenase (*FMO*) from *P. hybrida*. J. Fisetin pathway expressed in high-level *p*-CA strain ST2645; flavonoid 3′-monooxygenase (*FMO*) from *P. hybrida*. The strains were cultivated in FIT medium for 72 h, the mean value of extracellular concentration of compounds was calculated from five biological replicates.

this is indicative of a compound with a molecular formula of C15H10O6.

3.5. Improving fisetin production via heterologous pathway optimization

The strains designed to produce fisetin, accumulated significant amounts of quercetin. It was hypothesized that more flux could be re-directed into fisetin by exploiting the metabolic channeling effect, which had proven effective in other studies (Albertsen et al., 2011; Stahlhut et al., 2015). A fusion of CHS and CHR proteins was overexpressed in the fisetin-producing strain ST5074, resulting in ST5401. A control strain, ST5402, expressing an additional copy of non-fused *CHS* and *CHR* was constructed as well. Both strains produced higher titer of fisetin than the parental strain: strain ST5401 produced 2.11 ± 0.26 mg L^{-1} and strain ST5402 produced 2.29 ± 0.07 mg L^{-1} in comparison to 1.65 ± 0.01 mg L^{-1} for the parental strain ST5074 (Fig. 3A and B). As the competing by-product, quercetin, accumulated to the same concentration as in the strain without additional copies of *CHS* and *CHR*, the ratio of the product (fisetin) to by-product (quercetin) was slightly improved. However, the fusion clearly did not provide an additional advantage in comparison to overexpression of separate enzymes, and further work is needed to optimize the linkage between the two proteins.

The strains engineered for liquiritigenin, resokaempferol and fisetin production accumulated significant amounts of by-products. Particularly obtaining the products in the reduced branch was difficult and was always accompanied by production of non-reduced analogues. By overexpressing an extra copy of chalcone synthase *CHS* and chalcone reductase *CHR*, fisetin titer was increased from 1.65 ± 0.10 mg L^{-1} to 2.29 ± 0.07 mg L^{-1}. Clearly, further improvement of chalcone reductase is needed to obtain the reduced flavonoids.

When assembling novel heterologous pathways for production of the complex metabolites, it is important to engineer (or isolate) a microbial host with a sufficient pool of precursor metabolites for a given product and to ensure balanced enzymatic activities of the multistep metabolic pathways in order to avoid accumulation of intermediates and by-products (Venugopalan et al., 2016; Badle et al., 2014). Therefore, several engineered platform strains with different production capacities for production of flavonoids precursor *p*-coumaric acid were tested. In all cases, when the strains with improved flux towards *p*-coumaric acid via TAL route were implemented, an improvement in production of the downstream flavonoids was observed.

The accumulation of *p*-coumaric acid was common for all the engineered strains. The accumulation of this precursor indicates a limiting step for the conversion of *p*-coumaric acid into *p*-coumaroyl-CoA. Previous research reported the same limiting step in *E. coli* and yeast; they associated the accumulation of *p*-coumaric acid to the lack of malonyl-CoA or low activity of the *4CL* for conversion of *p*-coumaric acid into *p*-coumaroyl-CoA (Stahlhut et al., 2015; Koopman et al., 2012). To overcome this limitation, other natural or engineered variants of *4CL* can be tested and the supply of malonyl-CoA can be improved (Shi et al., 2014). Another possibility for improvements could be testing several different *S. cerevisiae* strain backgrounds, as miniature genetic and phenotypic differences might result in significant differences of the final yields of phytochemicals and biofuels (Strucko et al., 2015; Pereira et al., 2014). In higher plants, flavonoid biosynthetic enzymes are co-localized and assembled in protein complexes and the metabolic channeling effect decreases formation of by-products. In analogy, compartmentalizing or scaffolding the flavonoid biosynthetic enzymes in yeast may have a positive effect on the enzymatic activity and therefore on flavonoids production

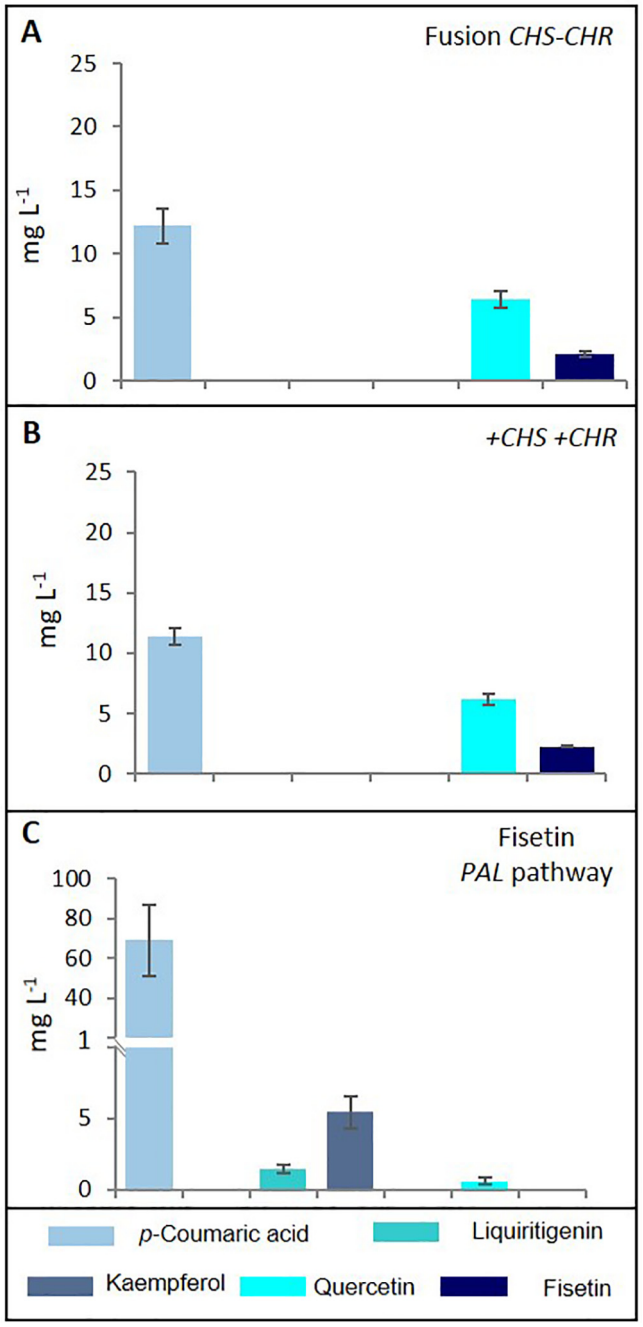

Fig. 3. Strains engineered for the optimized biosynthesis of fisetin. A. ST5401, fisetin producer strain (ST5075) with an additional copy of fused *CHS* and *CHR* B. ST5402, fisetin producer strain (ST5075) with an additional copy of *CHS* and *CHR*. C. Strain ST4972 engineered for biosynthesis of fisetin using the PAL pathway. The background strain for strains ST5401 and ST5402 was strain ST5074. The strains were cultivated in FIT medium for 72 h, the mean value of extracellular concentration of compounds was calculated from five biological replicates.

(Jeon et al., 2015; Avalos et al., 2013; Woolston et al., 2013; Dueber et al., 2009). Further studies are needed on kinetic regulation of the flux through the flavonoids pathway, on the degradation and secretion of flavonoids.

3.6. Biosynthesis of flavonoid via phenylalanine

Several studies have previously demonstrated that *p*-coumaric acid, the first intermediate of *de novo* flavonoid pathway, can be synthesized in *S. cerevisiae* via two routes: through tyrosine

ammonia-lyase TAL or phenylalanine ammonia-lyase PAL (Koopman et al., 2012; Li et al., 2015). In this study, the capacity of TAL and PAL routes to supply metabolic precursors for flavonoid production was compared. For this, a strain producing *p*-coumaric acid via PAL route was constructed (ST4757). The strain featured overexpression of *CYB5 from S. cerevisiae* and *PAL2, ATR2* and *C4H* and from *Arabidopsis thaliana*. The pathway for biosynthesis of fisetin was introduced into this strain as the next step. The pathway was analogous to the one described above in ST5074. Interestingly, HPLC analysis of the resulting final PAL-based strain (ST4972) revealed a different metabolic profile (Fig. 3C) as compared to the corresponding TAL-based strain. More specifically, a 5.7-fold higher accumulation of *p*-coumaric acid (70 mg L^{-1}) was observed, while fisetin was only found in trace amounts and could not be quantified.

Surprisingly, when PAL route was applied for the production of fisetin, a much higher accumulation of *p*-coumaric acid was observed (69.07 ± 17.81 mg L^{-1} instead of 12.63 ± 0.76 mg L^{-1}), the production of quercetin was lower and there was no production of fisetin. Another surprising discovery was the relatively high titer of kaempferol (26.57 ± 2.66 mg L^{-1}), despite the parental strain produced only 1.55 ± 0.13 mg L^{-1} of kaempferol precursor, naringenin. This phenomenon could be explained by intracellular degradation of naringenin, its instability in the medium or lower secretion of kaempferol (Mora-Pale et al., 2013; Du et al., 2010).

4. Conclusions

This work presents a proof-of-concept biosynthesis of flavonoids in engineered yeast cell factories. An array of yeast strains expressing heterologous flavonoid metabolic pathways was successfully developed. The strains contained up to eight genes, where some of the strains produced significant flavonoid titers in double-digit mg L^{-1} range. Moreover, the study demonstrated that flavonoids can be synthesized via two different precursor-supplying routes, via tyrosine ammonia-lyase or phenylalanine ammonia-lyase. The compounds quercetin and kaempferol were the ones with the highest extracellular concentrations detected in this study. This study is the first report on the biosynthesis of resokaempferol and fisetin in yeast.

Acknowledgements

This work was financed by the Novo Nordisk Foundation. The authors thank Dr. Vratislav Stovicek for providing the integrative vectors for stable gene expression and Dr. Mingji Li for providing the parts for the construction of the PAL pathway. TS, SS and JF have been funded by BacHBerry (European Commission, the 7th Framework Programme, Project No. FP7-613793) and ERA-IB project DeYeastLibrary (https://www.patil.embl.de/deyeastlibrary).

Appendix A. Supplementary data

Supplementary data associated with this article can be found, in the online version, at http://dx.doi.org/10.1016/j.biortech.2017.06.043.

References

Albertsen, L., Chen, Y., Bach, L.S., Rattleff, S., Maury, J., Brix, S., Nielsen, J., Mortensen, U.H., 2011. Diversion of flux toward sesquiterpene production in *Saccharomyces cerevisiae* by fusion of host and heterologous enzymes. Appl. Environ. Microbiol. 77, 1033–1040. http://dx.doi.org/10.1128/AEM.01361-10.

Avalos, J.L., Fink, G.R., Stephanopoulos, G., 2013. Compartmentalization of metabolic pathways in yeast mitochondria improves the production of branched-chain alcohols. Nat. Biotechnol. 31, 335–341. http://dx.doi.org/10.1038/nbt.2509.

Badle, S.S., Jayaraman, G., Ramachandran, K.B., 2014. Ratio of intracellular precursors concentration and their flux influences hyaluronic acid molecular weight in Streptococcus zooepidemicus and recombinant Lactococcus lactis. Bioresour. Technol. 163, 222–227. http://dx.doi.org/10.1016/j.biortech.2014.04.027.

Bulzomi, P., Galluzzo, P., Bolli, A., Leone, S., Acconcia, F., Marino, M., 2012. The pro-apoptotic effect of quercetin in cancer cell lines requires ERβ-dependent signals. J. Cell. Physiol. 227, 1891–1898. http://dx.doi.org/10.1002/jcp.22917.

Caltagirone, S., Rossi, C., Poggi, A., Ranelletti, F.O., Natali, P.G., Brunetti, M., Aiello, F. B., Piantelli, M., 2000. Flavonoids apigenin and quercetin inhibit melanoma growth and metastatic potential. Int. J. Cancer 87, 595–600. http://dx.doi.org/10.1002/1097-0215(20000815)87:4**595: AID-IJC21>3.0.CO;2-5.

Chen, A.Y., Chen, Y.C., 2013. A review of the dietary flavonoid, kaempferol on human health and cancer chemoprevention. Food Chem. 138, 2099–2107. http://dx.doi.org/10.1016/j.foodchem.2012.11.139.

Choi, E.M., 2012. Liquiritigenin isolated from Glycyrrhiza uralensis stimulates osteoblast function in osteoblastic MC3T3-E1 cells. Int. Immunopharmacol. 12, 139–143. http://dx.doi.org/10.1016/j.intimp.2011.11.003.

Chou, R.H., Hsieh, S.C., Yu, Y.L., Huang, M.H., Huang, Y.C., Hsieh, Y.H., 2013. Fisetin inhibits migration and invasion of human cervical cancer cells by down-regulating urokinase plasminogen activator expression through suppressing the p38 MAPK-dependent NF-KB signaling pathway. PLoS One 8, 1–12. http://dx.doi.org/10.1371/journal.pone.0071983.

Crozier, A., Lean, M.E.J., McDonald, M.S., Black, C., 1997. Quantitative analysis of the flavonoid content of commercial tomatoes, onions, lettuce, and celery. J. Agric. Food Chem. 45, 590–595. http://dx.doi.org/10.1021/jf960339y.

Currais, A., Prior, M., Dargusch, R., Armando, A., Ehren, J., Schubert, D., Quehenberger, O., Maher, P., 2014. Modulation of p25 and inflammatory pathways by fisetin maintains cognitive function in Alzheimer's disease transgenic mice. Aging Cell 13, 379–390. http://dx.doi.org/10.1111/acel.12185.

Cushnie, T.P.T., Lamb, A.J., 2011. Recent advances in understanding the antibacterial properties of flavonoids. Int. J. Antimicrob. Agents 38, 99–107. http://dx.doi.org/10.1016/j.ijantimicag.2011.02.014.

Du, B., Sharma, L.N., Becker, C., Chen, S., Mowery, R.A., Van Walsum, G.P., Chambliss, C.K., 2010. Effect of varying feedstock – pretreatment chemistry combinations on the formation and accumulation of potentially inhibitory degradation products in biomass hydrolysates. Biotechnol. Bioeng. http://dx.doi.org/10.1002/bit.22829.

Dueber, J.E., Wu, G.C., Malmirchegini, G.R., Moon, T.S., Petzold, C.J., Ullal, A.V., Prather, K.L.J., Keasling, J.D., 2009. Synthetic protein scaffolds provide modular control over metabolic flux. Nat. Biotechnol. 27, 5–8. http://dx.doi.org/10.1038/nbt.1557.

Gietz, B.R.D., Woods, R.A., 2002. Transformation of yeast by lithium acetate/single-stranded carrier dna/polyethylene glycol method. Methods Enzymol. 350, 87–96.

Grotewold, E., 2006. The Science of Flavonoids. Springer Science Business Media Inc, New York.

Hämäläinen, M., Nieminen, R., Vuorela, P., Heinonen, M., Moilanen, E., 2007. Anti-inflammatory effects of flavonoids: genistein, kaempferol, quercetin, and daidzein inhibit STAT-1 and NF-κB activations, whereas flavone, isorhamnetin, naringenin, and pelargonidin inhibit only NF-κB activation along with their inhibitory effect on iNOS expression and NO production in activated macrophages. Mediators Inflamm. http://dx.doi.org/10.1155/2007/45673.

Hertog, M.G., Hollman, P.C., Katan, M.B., 1992. Content of potentially anticarcinogenic flavonoids of 28 vegetables and 9 fruits commonly consumed in The Netherlands. J. Agric. Food Chem. 40, 2379–2383. http://dx.doi.org/10.1021/jf00024a011.

Jeon, S.D., Kim, S.J., Park, S.H., Choi, G.W., Han, S.O., 2015. Hydrolytic effects of scaffolding proteins CbpB and CbpC on crystalline cellulose mediated by the major cellulolytic complex from Clostridium cellulovorans. Bioresour. Technol. 191, 505–511. http://dx.doi.org/10.1016/j.biortech.2015.02.071.

Koopman, F., Beekwilder, J., Crimi, B., van Houwelingen, A., Hall, R.D., Bosch, D., van Maris, A.J., Pronk, J.T., Daran, J.-M., 2012. *De novo* production of the flavonoid naringenin in engineered *Saccharomyces cerevisiae*. Microb. Cell Fact. 11, 155. http://dx.doi.org/10.1186/1475-2859-11-155.

Leonard, E., Yan, Y., Koffas, M.A.G., 2006. Functional expression of a P450 flavonoid hydroxylase for the biosynthesis of plant-specific hydroxylated flavonols in *Escherichia coli*. Metab. Eng. 8, 172–181. http://dx.doi.org/10.1016/j.ymben.2005.11.001.

Li, M., Kildegaard, K.R., Chen, Y., Rodriguez, A., Borodina, I., Nielsen, J., 2015. *De novo* production of resveratrol from glucose or ethanol by engineered *Saccharomyces cerevisiae*. Metab. Eng. 32, 1–11. http://dx.doi.org/10.1016/j.ymben.2015.08.007.

Li, M., Schneider, K., Kristensen, M., Borodina, I., Nielsen, J., 2016. Engineering yeast for high-level production of stilbenoid antioxidants. Sci. Rep. http://dx.doi.org/10.1038/srep36827. 6:36827.

Liu, Y., Xie, S., Wang, Y., Luo, K., Wang, Y., Cai, Y., 2012. Liquiritigenin inhibits tumor growth and vascularization in a mouse model of HeLa cells. Molecules 17, 7206–7216. http://dx.doi.org/10.3390/molecules17067206.

Luthria, D.L., 2012. Optimization of extraction of phenolic acids from a vegetable waste product using a pressurized liquid extractor. J. Funct. Foods 4, 842–850. http://dx.doi.org/10.1016/j.jff.2012.06.001.

Maher, P., Dargusch, R., Bodai, L., Gerard, P.E., Purcell, J.M., Lawrence Marsh, J., 2011. Erk activation by the polyphenols fisetin and resveratrol provides neuroprotection in multiple models of Huntington's disease. Hum. Mol. Genet. 20, 261–270. http://dx.doi.org/10.1093/hmg/ddq460.

Makris, D.P., Boskou, G., Andrikopoulos, N.K., 2007. Recovery of antioxidant phenolics from white vinification solid by-products employing water/ethanol mixtures. Bioresour. Technol. 98, 2963–2967. http://dx.doi.org/10.1016/j.biortech.2006.10.003.

Matharu, A.S., De Melo, E.M., Houghton, J.A., 2016. Opportunity for high value-added chemicals from food supply chain wastes. Bioresour. Technol. 215, 123–130. http://dx.doi.org/10.1016/j.biortech.2016.03.039.

Miean, K.H., Mohamed, S., 2001. Flavonoid (myricetin, quercetin, kaempferol, luteolin, and apigenin) content of edible tropical plants. J. Agric. Food Chem. 49, 3106–3112.

Mikkelsen, M.D., Buron, L.D., Salomonsen, B., Olsen, C.E., Hansen, B.G., Mortensen, U. H., Halkier, B.A., 2012. Microbial production of indolylglucosinolate through engineering of a multi-gene pathway in a versatile yeast expression platform. Metab. Eng. 14 (2), 104–111. http://dx.doi.org/10.1016/j.ymben.2012.01.006.

Mirabella, N., Castellani, V., Sala, S., 2014. Current options for the valorization of food manufacturing waste: a review. J. Clean. Prod. 65, 28–41. http://dx.doi.org/10.1016/j.jclepro.2013.10.051.

Mora-pale, M., Sanchez-rodriguez, S.P., Linhardt, R.J., Dordick, J.S., Koffas, M.A.G., 2013. Metabolic engineering and in vitro biosynthesis of phytochemicals and non-natural analogues. Plant Sci. 210, 10–24. http://dx.doi.org/10.1016/j.plantsci.2013.05.005.

Mukhtar, E., Adhami, V.M., Sechi, M., Mukhtar, H., 2015. Dietary flavonoid fisetin binds to β-tubulin and disrupts microtubule dynamics in prostate cancer cells. Cancer Lett. 367, 173–183. http://dx.doi.org/10.1016/j.canlet.2015.07.030.

Paganga, G., Miller, N., Rice-Evans, C.A., 1999. The polyphenolic content of fruit and vegetables and their antioxidant activities. What does a serving constitute? Free Radical Res. 30, 153–162. http://dx.doi.org/10.1080/10715769900300161.

Pereira, F.B., Romaní, A., Ruiz, H.A., Teixeira, J.A., Domingues, L., 2014. Industrial robust yeast isolates with great potential for fermentation of lignocellulosic biomass. Bioresour. Technol. 161, 192–199. http://dx.doi.org/10.1016/j.biortech.2014.03.043.

Pfaltzgraff, L.A., De, M., Cooper, E.C., Budarin, V., Clark, H., 2013. Food waste biomass: a resource for high-value Chemicals. Green. Chem. 15, 307–314. http://dx.doi.org/10.1039/c2gc36978h.

Raza, S.S., Khan, M.M., Ahmad, A., Ashafaq, M., Islam, F., Wagner, A.P., Safhi, M.M., Islam, F., 2013. Neuroprotective effect of naringenin is mediated through suppression of NF-kB signaling pathway in experimental stroke. Neuroscience 230, 157–171. http://dx.doi.org/10.1016/j.neuroscience.2012.10.041.

Rodriguez, A., Kildegaard, K.R., Li, M., Borodina, I., Nielsen, J., 2015. Establishment of a yeast platform strain for production of p-coumaric acid through metabolic engineering of aromatic amino acid biosynthesis. Metab. Eng. 31, 181–188. http://dx.doi.org/10.1016/j.ymben.2015.08.003.

Routray, W., Orsat, V., 2012. Microwave-assisted extraction of flavonoids: a review. Food Bioprocess Technol. 5, 409–424. http://dx.doi.org/10.1007/s11947-011-0573-z.

Santos, C.N.S., Koffas, M., Stephanopoulos, G., 2011. Optimization of a heterologous pathway for the production of flavonoids from glucose. Metab. Eng. 13, 392–400. http://dx.doi.org/10.1016/j.ymben.2011.02.002.

Shi, S., Chen, Y., Siewers, V., 2014. Improving production of malonyl coenzyme A-derived metabolites 5, 1–8. doi:10.1128/mBio.01130-14.

Stahlhut, S.G., Siedler, S., Malla, S., Harrison, S.J., Maury, J., Neves, A.R., Forster, J., 2015. Assembly of a novel biosynthetic pathway for production of the plant flavonoid fisetin in *Escherichia coli*. Metab. Eng. 31, 84–93. http://dx.doi.org/10.1016/j.ymben.2015.07.002.

Stovicek, V., Borja, G.M., Forster, J., Borodina, I., 2015. EasyClone 2.0: expanded toolkit of integrative vectors for stable gene expression in industrial *Saccharomyces cerevisiae* strains. J. Ind. Microbiol. Biotechnol. 42, 1519–1531. http://dx.doi.org/10.1007/s10295-015-1684-8.

Strucko, T., Magdenoska, O., Mortensen, U.H., 2015. Benchmarking two commonly used *Saccharomyces cerevisiae* strains for heterologous vanillin-β-glucoside production. Metab. Eng. Commun. 2, 99–108. http://dx.doi.org/10.1016/j.meteno.2015.09.001.

Trantas, E., Panopoulos, N., Ververidis, F., 2009. Metabolic engineering of the complete pathway leading to heterologous biosynthesis of various flavonoids and stilbenoids in *Saccharomyces cerevisiae*. Metab. Eng. 11, 355–366. http://dx.doi.org/10.1016/j.ymben.2009.07.004.

Venugopalan, A., Potunuru, U.R., Dixit, M., Srivastava, S., 2016. Effect of fermentation parameters, elicitors and precursors on camptothecin production from the endophyte Fusarium solani. Bioresour. Technol. 213, 311–318. http://dx.doi.org/10.1016/j.biortech.2016.05.023.

Wang, Y., Chen, S., Yu, O., 2011. Metabolic engineering of flavonoids in plants and microorganisms. Appl. Microbiol. Biotechnol. 91, 949–956. http://dx.doi.org/10.1007/s00253-011-3449-2.

Wedick, N.M., Pan, A., Cassidy, A., Rimm, E.B., Sampson, L., Rosner, B., Willett, W., Hu, F.B., Sun, Q., Van Dam, R.M., 2012. Dietary flavonoid intakes and risk of type 2 diabetes in US men and women. Am. J. Clin. Nutr. 95, 925–933. http://dx.doi.org/10.3945/ajcn.111.028894.

Woelfle, U., Simon-Haarhaus, B., Merfort, I., Schempp, C.M., 2010. *Reseda luteola* L. extract displays antiproliferative and pro-apoptotic activities that are related to its major flavonoids. Phytother. Res. 24, 1033–1036. http://dx.doi.org/10.1002/ptr.3069.

Woolston, B.M., Edgar, S., Stephanopoulos, G., 2013. Metabolic engineering: past and future. Annu. Rev. Chem. Biomol. Eng. 4, 259–288. http://dx.doi.org/10.1146/annurev-chembioeng-061312-103312.